An X-ray photoelectron spectroscopic perspective for the evolution of O-containing structures in char during gasification

Shuai Wang, Liping Wu, Xun Hu, Lei Zhang, Kane M O'Donnell, Craig E Buckley and Chun-Zhu Li*

Fuels and Energy Technology Institute, Curtin University of Technology, GPO Box U1987, Perth, WA 6845, Australia

Submitted to

Fuel Processing Technology

For consideration for publication

Oct 2017

*Corresponding author: chun-zhu.li@curtin.edu.au; telephone: +61 8 9266 1131; facsimile: +61 8 9266 1138

Abstract

The purpose of this study is to investigate the evolution of O-containing structures of char during gasification. Mallee wood (4.75-5.60 mm) from Western Australia was gasified in a fluidised-bed reactor at 600-900 ˚C in O-containing (pure CO_2, 15% H_2O-Ar) and non-O-containing atmospheres (15% H_2-Ar). X-ray photoelectron spectroscopy (XPS) was applied to obtain detailed information about the nature of oxygen bonding with carbon as well as the content of oxygen species in char. The similar O/C ratio of char from XPS and elemental analysis indicated the relative chemical uniformity between char surface and char matrix. The deconvolution results of the O 1s spectra showed that the reactivity of the inherent aromatic C-O structure was much higher than that of the aromatic C=O structure during gasification. The amount of aromatic C-O structure left in char during gasification in non-O-containing atmosphere was lower than that in O-containing atmosphere while the consumption of aromatic C=O structure was proportional to the progress of gasification, regardless of the atmosphere. The newly formed C-O structure in char during the gasification in the O-containing atmosphere was likely to be responsible for the high gasification reactivity. The well-dispersed alkali earth metallic species could be carbonated to form $CaCO_3$ and $MgCO_3$ on char surface once the char was exposed to CO_2 at 900 ˚C.

Keywords: X-ray photoelectron spectroscopy; Oxygen-containing structure; Char oxygenation; Gasification; Biomass

1. Introduction

Char gasification is the rate-limiting step for the overall solid fuel gasification process [1,2]. There are a few important inter-related factors influencing the char gasification rate [3]. Firstly, the inherent alkali and alkaline earth metallic (AAEM) species in char can act as excellent catalysts for char gasification [3]. The presence of highly dispersed AAEM species can significantly speed up the gasification reaction, affect the properties of pyrolysis products, and have a great impact on the evolution of the char structure [4-8]. Secondly, the transformation of aromatic ring systems in char will greatly influence char reactivity during gasification. It has become clear that the small ring systems (equivalent to 3-5 fused benzene rings) are preferentially consumed while the large ones (more than 6 fused rings) are preferentially left and/or formed during gasification, making the residual char more condensed and hard to gasify [9-13]. Thirdly, the O-containing functional groups in char will also greatly influence the gasification rate to some extent, especially for the gasification of the low-rank fuels at low temperature. It is believed that some O-containing structures in char are responsible for enhancing the char gasification rate [4,9]. For a better understanding of the gasification mechanisms, the changes in char structure, especially the evolution of O-containing structures, must be quantified during gasification.

FT-Raman spectroscopy has been demonstrated to be a powerful analytical method to characterise the evolution of aromatic ring systems in char during gasification due to its outstanding ability to respond to the non-polar bond vibration [14-20]. However, only limited information can be obtained from the Raman spectra about the changes of O-containing structures in char, especially the changes in the

chemical bonding between oxygen and carbon during gasification. The total Raman intensity can be used as an indication of the relative amount of the O-containing functional groups in char that can induce a resonance effect between oxygen and the aromatic ring to which it is connected [14]. Not all oxygen species in char could have the resonance effect with the aromatic rings. Fourier transform infrared (FT-IR) spectroscopy may be responsive to a wide range of O-containing structures in char. However, FT-IR spectroscopy would have some potential difficulties within the context of tracing the changes in the O-containing structures during gasification. For example, the absorption coefficients may vary by a magnitude or more from one type of O-containing functional group to another.

Therefore, other techniques must be applied to study O-containing functional groups in char and provide useful information on the evolution of O-containing structures in char during gasification. X-ray photoelectron spectroscopy (XPS) has proved to be one of the most powerful tools in detecting the surface structure of carbonaceous materials [21-24]. Although the validity of XPS analysis is limited to determining the surface structure of material, its high sensitivity to the chemical nature of atomic species has made it extensively developed as a useful technique for identifying the structural features of different types of carbon materials [25,26]. In addition, the ability to identify elemental bonding states has make it widely used in determining the organic functional group composition of char through a detailed analysis of the high-resolution band of each elements [27,28]. Another important feature of XPS spectroscopy is the unchanged sensitivity of oxygen regardless of its chemical structures/functionality. This greatly facilitates the relative quantification of various classes of O-containing structures simply based on the measured peak areas.

The purpose of this study is to investigate the effects of gasification temperature and gasification atmosphere on the evolution of O-containing structures in char. XPS has been applied to characterise oxygen species in chars produced from the gasification of mallee wood at 600-900 ˚C in three different atmospheres (pure CO_2, 15% H_2O-Ar, 15% H_2-Ar). The high-resolution O 1s peak of the XPS spectra were further deconvoluted in order to gain insights into the nature of the bonding between oxygen and carbon in addition to the determination of the contents of oxygen in char. Our data provided further insight into the char gasification mechanisms.

2. Experimental

2.1 Biomass gasification

Mallee wood in the size range of 4.75-5.60 mm from Western Australia was used as the feedstock in this research. The proximate analysis of the sample results in a 0.9% ash yield and 81.6% volatiles yield, and the elemental analysis of the sample determined 48.2% C, 6.1% H, 0.2% N and 45.5% O (wt%, dry and ash-free basis).

A fluidised-bed quartz reactor [29] was used to carry out the biomass gasification experiments. Approximately 2 g of biomass (weighed accurately) was pre-loaded into the feeder. Before feeding, the reactor was heated to the target temperature with the flow of Ar through the reactor. The feeding of biomass into the reactor commenced with the help of an electrical vibrator. When the feeding was finished, the reactor was held for 20 minutes to ensure that all volatiles had been released. The reaction gas was switched from Ar to the gasifying agent. For gasification in the steam atmosphere, it was 15% steam balanced with Ar. For gasification in the H_2 atmosphere, it was 15% H_2 balanced with Ar. For gasification in the CO_2 atmosphere,

pure CO_2 was used. After 4 minutes of holding in the gasification atmosphere, the reactor was lifted out of the furnace and cooled down naturally with Ar flowing into the reactor instead of the gasifying agents. After each experiment, the collected char sample was placed in sealed vials and stored in a freezer to avoid further oxidation by the ambient oxygen.

2.2 Char characterisation

XPS spectra were acquired with a Kratos AXIS Ultra DLD XPS spectrometer equipped with a Al-Kα X-ray monochromator (photon energy 1486.7 eV). XPS measurements were carried out under ultra-high vacuum conditions ($< 2.0\times10^{-10}$ mbar) at room temperature. The survey scans were taken across the sample with binding energy from 1400 to 0 eV to determine all elements present in char. A pass energy of 40 eV was used for the collection of high-resolution spectrum of each of the selected elements.

Elemental analysis was carried out using a FLASH 200 elemental analyser. Char sample was firstly ground to powder and then about 2.5 mg (weighed accurately) sample was loaded into a tin capsule. The tin capsule was folded and placed in the autosampler for analysis.

3. Deconvolution and band assignment of the XPS spectra

Data processing of the acquired XPS spectra of chars was performed using the CasaXPS peak fitting software. The binding energy of the original XPS spectra was calibrated with respect to the carbon component of the C 1s peak at 284.5 eV. The spectra were curve-fitted after linear pre-edge and Shirley background subtraction,

using mixed Gaussian-Lorentzian bands. The position and assignment of the bands in the O 1s spectra are briefly summarised in Table 1.

Table 1 Summary of peak/band assignment.

Spectra	Band position, eV	Description	References
O 1s	531.4	Aromatic C=O structure	11,27,30-32
	533.4	Aromatic C-O structure	23,27,31-33
	536.0	Absorbed O_2	11,23

The curve-fitting of the high-resolution O 1s spectra was taken in the range between 528.0 and 539.0 eV. The broadening of the O 1s spectra means large varieties of O-containing structures presented in char. Based on the XPS spectra of some model compounds [11,30,31], one band at 531.3 eV was assigned to the C=O (aromatic) functional groups such as benzoquinone-type structure in char. Another band at 531.6 eV was attributed to the R-(C=O)-C (aromatic) functional groups such as aromatic ketone or carbonyl structure in char [27,31,32]. It is clear that these two kinds of O-containing functional groups have very close binding energies and they cannot be reliably distinguished through the curve-fitting procedure. Therefore, in this study, the band at 531.4 eV was assigned to all aromatic C=O structures in char. Since it represents more than one type of structure the band is broader than that for a pure model compound.

On the high binding energy side, one band at the position 533.2 eV was attributed to oxygen inside the carbon ring such as epoxide or furan type structure in char [27,31,33]. Another band at 533.3 eV was assigned to the O-C (aromatic) structure such as phenol or diphenyl ether [23,31,32]. Moreover, the band located at 533.6 eV was assigned to the O-(C=O)-C (aromatic) functional group such as carboxyl structure in char [31]. Similarly, because of the close binding energies among these

three oxygen-carbon structures and the complexity of O-contaning functional groups in char, the band at 533.4 eV was assigned to all aromatic C-O structures in char.

In addition to the two main bands assigned above, another weak peak appearing at 536.0 eV was identified as the absorbed O_2 existing on char surface [11,23].

A typical example of the spectral deconvolution/curve-fitting of the high-resolution O 1s peak of char using three bands is shown in Fig. 1. Similar success of curve-fitting can also be achieved for all other char samples investigated in this study.

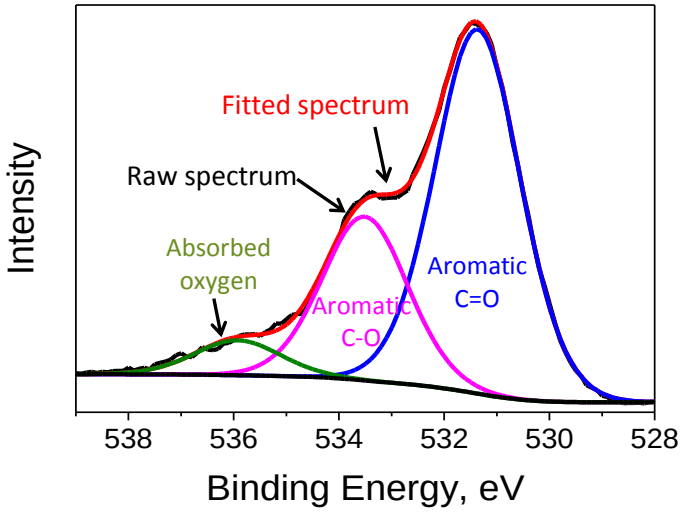

Fig. 1. Spectral deconvolution of a XPS O 1s peak of char from the gasification of mallee wood at 700 ˚C in 15% H_2O balanced with Ar.

4. Results and discussion

4.1 Char yield

The gasification of mallee woody biomass was carried out at different temperatures ranging from 600 to 900 ˚C in three gasifying agents (pure CO_2, 15% H_2O-Ar, 15% H_2-Ar). Fig. 2 shows the char yields as a function of gasification temperature in three gasifying atmospheres. As expected, the char yield decreased

with increasing temperature because of the enhanced thermal cracking and gasification reaction. In addition, for different gasification atmospheres, when the temperature was below 700 ˚C, there was not much difference in the char yield, indicating that the main reaction was pyrolysis at this stage. However, when the temperature was higher than 700 ˚C, the gasification reaction became fierce and the gasification in CO_2 proceeded the fastest among the three atmospheres. As expected, the conversion of char proceeded the slowest during the gasification in H_2 atmosphere, confirming that the char-H_2 reaction was much slower than the char-H_2O and char-CO_2 reactions [4,16].

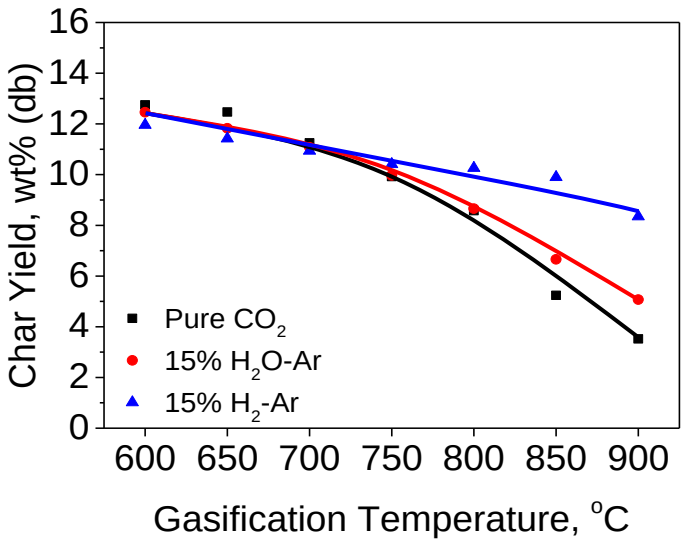

Fig. 2. Char yield as a function of gasification temperature for mallee wood in pure CO_2, 15% H_2O balanced with Ar and 15% H_2 balanced with Ar.

4.2 Formation of carbonates during the gasification in CO_2 at 900 ˚C

According to our previous studies [15,34], the extensive volatilisation of Ca and Mg from char matrix during the gasification of Victorian brown coal in CO_2 at 900 ˚C in a fluidised-bed reactor took place because of the formation and aggregation of carbonates on char surface. Ca and Mg species were present as the carboxyl-bound

cations, and would retain their high dispersion during fast pyrolysis even at high temperature (up to 950 ˚C) [6,34]. Once the char was exposed to CO_2 at 900 ˚C, the well-dispersed alkali earth metallic species could be carbonated to form $CaCO_3$ and $MgCO_3$ on the char surface [34,35,36].

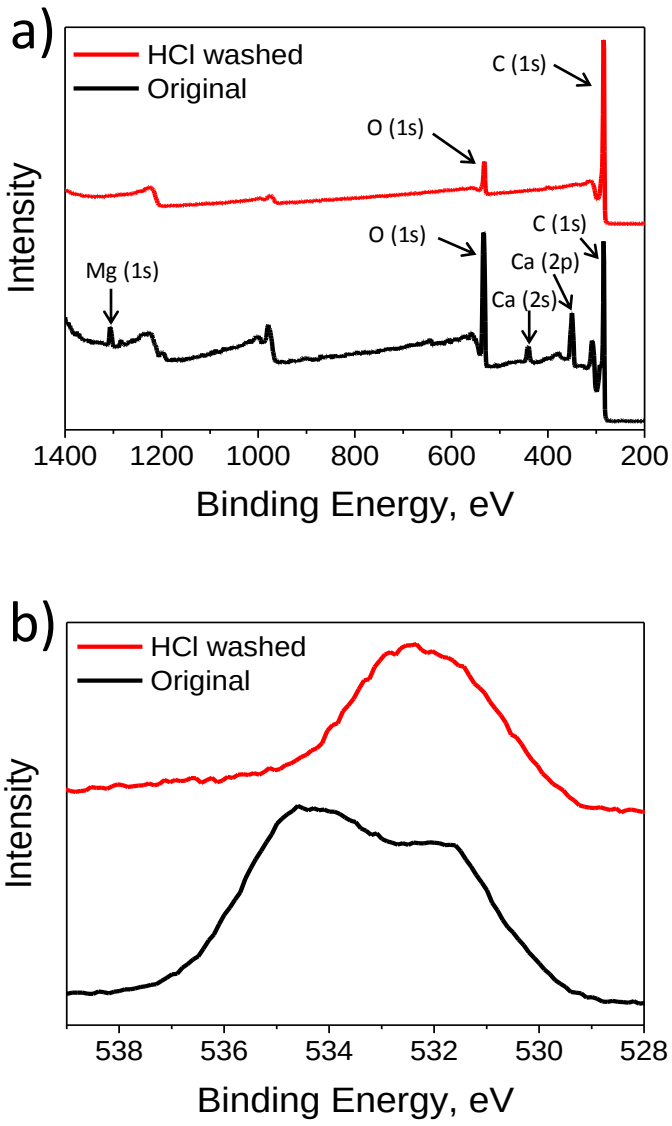

Fig. 3. Effects of acid washing on the XPS spectra of (a) survey scan and (b) high-resolution of O 1s peak of the char from the gasification of mallee wood at 900 ˚C in pure CO_2.

This result was confirmed by the XPS analysis in this work. Fig. 3 shows the XPS spectra of the char from the gasification of mallee wood at 900 ˚C in pure CO_2. The high-resolution O 1s spectrum showed a clear peak located at 535.0 eV, which is the

position for carbonate structures [37]. In order to clarify the nature of this band, the char was washed with 0.2 M hydrochloric acid to remove the carbonates as well as the AAEM species on char surface. It can be seen from the survey scan that almost all Ca and Mg species were removed from the char, and the band in the range of 534.0-536.0 eV in the O 1s high-resolution spectrum disappeared after the acid-washing, indicating the formation of $CaCO_3$ and $MgCO_3$ during gasification in CO_2 at 900 ˚C. No clear carbonate peak can be seen in the O 1s high-resolution spectra of char from the gasification below 900 ˚C in pure CO_2.

4.3 Similarity in O/C ratio between surface and bulk analyses

In order to identify whether there were some differences in the contents of carbon and oxygen between the char surface and the char matrix, the results from elemental analysis were compared with those from XPS analysis. The contents of carbon and oxygen in char from XPS analysis were obtained by the calculation of total peak intensity and the relative sensitivity factors of each element. Due to the inability to detect the H element through the XPS analysis, the O/C ratio of char during gasification was used to compare the difference between surface and bulk analyses.

As is shown in Fig. 4, the O/C ratio of char obtained both from XPS and elemental analysis exhibited a decrease with the increasing gasification temperature, indicating the decline in the oxygen content of char during gasification at high temperature. More importantly, for a given temperature, the O/C ratios of char from XPS and elemental analysis were almost the same and the relative difference between these two analysis results was less than 6%, which means the whole char particle was chemically uniform and there was not much difference between the surface and char matrix. Although the XPS analysis cannot detect the H element in char, based on the

elemental analysis results, the content of H species in char was very little (less than 2%). Therefore, the XPS analysis can still be used as a characterisation method to indicate the concentration of carbon and oxygen species of the whole char particles during gasification.

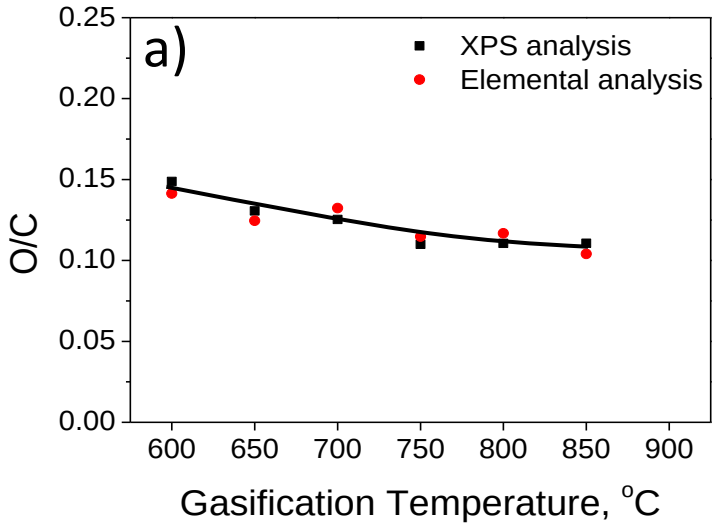

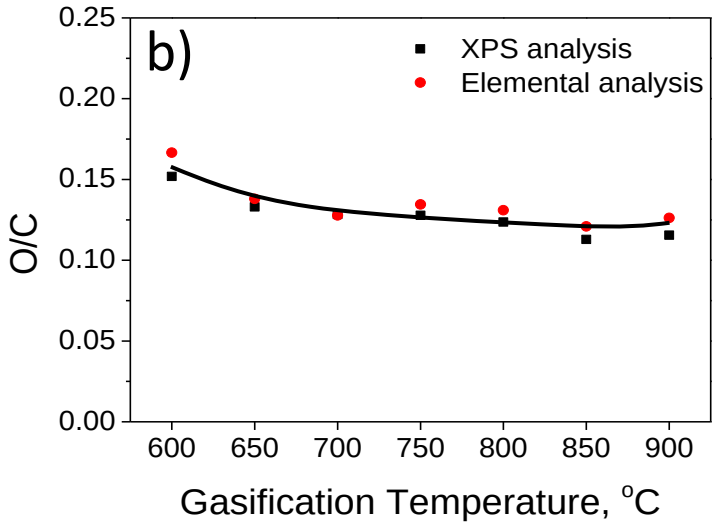

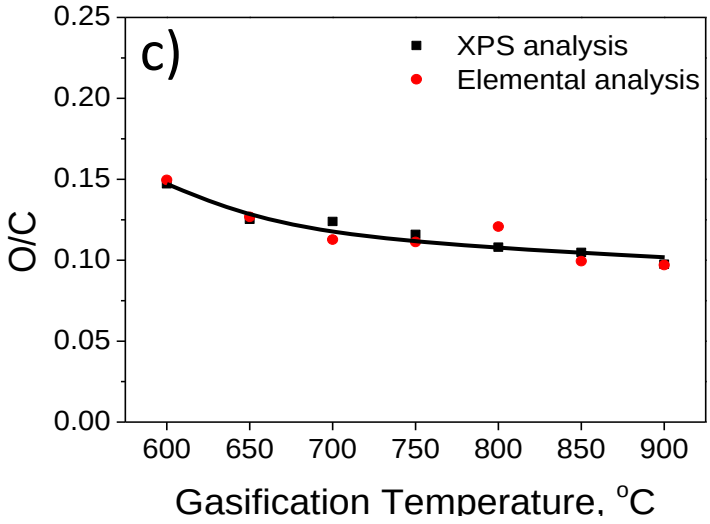

Fig. 4. The O/C ratios of chars as a function of gasification temperatures for mallee wood in (a) pure CO_2, (b) 15% H_2O balanced with Ar and (c) 15% H_2 balanced with Ar.

4.4 Relative distribution of chemical components in O 1s spectra

A clear trend for the changes in O-containing structure can be found through the deconvolution of O 1s spectra of chars. Fig. 5 illustrates the relative distribution of O-containing structures in O 1s high-resolution spectra. It can be seen that the distribution of aromatic C-O structures in the O 1s spectra continuously decreased with increasing gasification temperature, while an increasing trend was shown on the distribution of aromatic C=O structures in the O 1s spectra with increasing gasification temperature. The deconvolution result of O 1s spectra can only show the relative content of O-containing structures, in order to identify the exact amount of O-containing structures left in char during gasification, the absolute quantity of each chemical component should be calculated, which will be discussed in the following section.

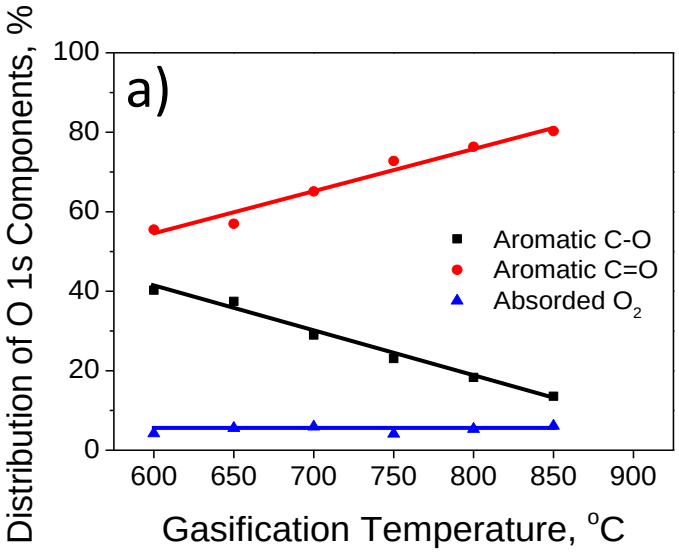

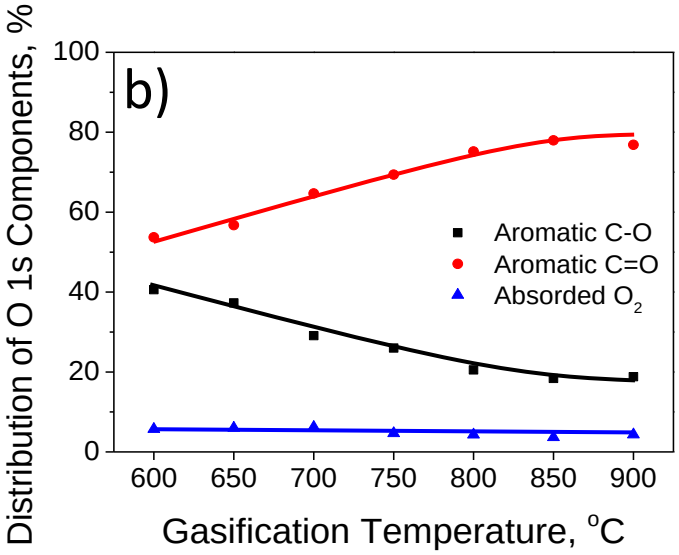

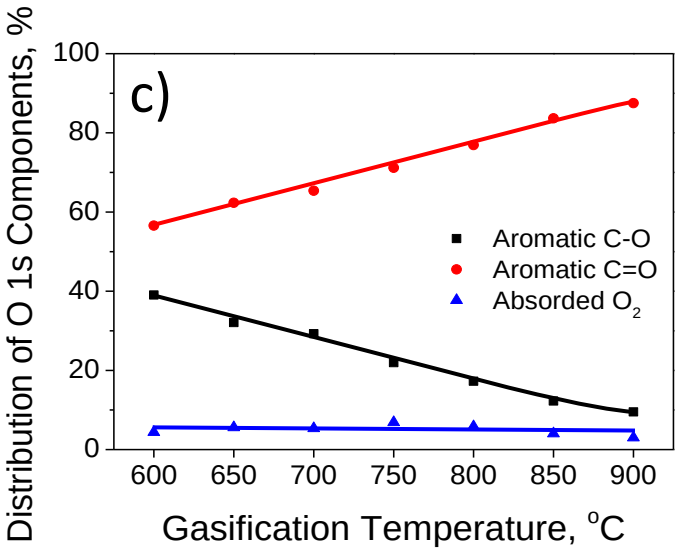

Fig. 5. Distribution of O-containing structure in O 1s spectra obtained by XPS analysis as a function of gasification temperatures for mallee wood in (a) pure CO_2, (b) 15% H_2O balanced with Ar and (c) 15% H_2 balanced with Ar.

4.5 Absolute amount of oxygen species in char during gasification

The absolute amount refers to the amount of a particular type of XPS-derived O-containing structure in char based on an initial gram of biomass (before gasification at each temperature). The absolute amounts of O-containing structure in char obtained by the XPS calculation results and the char yield of mallee wood during gasification are illustrated in Fig. 6.

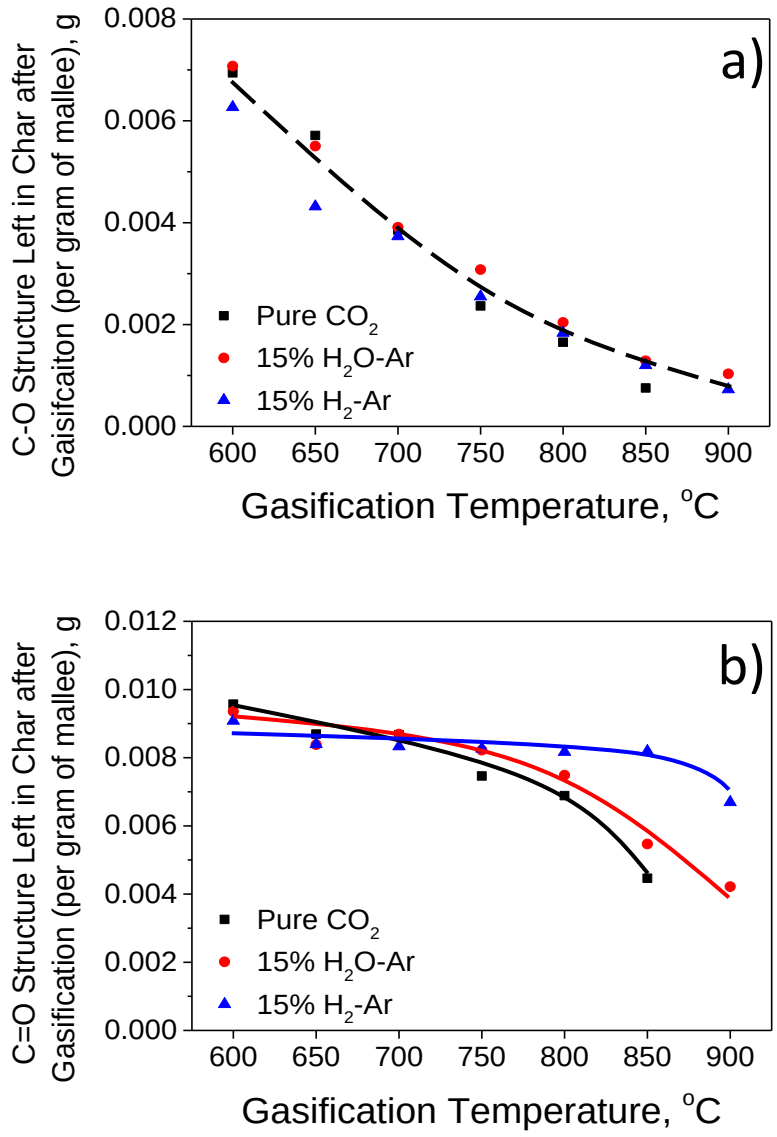

Fig. 6. Amount of (a) C-O structure and (b) C=O structure left in char after gasification based on per gram of mallee wood obtained by XPS analysis as a function of gasification temperatures.

291 It can be seen that there was a drastic decrease in the aromatic C-O structures in
292 char with increasing temperature for all three gasification atmospheres, indicating the
293 high reactivity of aromatic C-O structures during gasification. In addition, a clear
294 difference appeared for the amount of aromatic C=O structures left in char between
295 gasification in H_2 atmosphere and the O-containing atmosphere (CO_2, H_2O). The
296 amounts of C=O structures in char from the gasification in steam and in CO_2
297 continuously decreased with increasing temperature. However, such structure in
298 chars from the gasification in H_2 was almost constant when the gasification
299 temperature was below 900 ˚C. The char gasification in H_2 was quite slow and the
300 loss of O-containing structure was mainly because of the enhanced thermal cracking,
301 not the gasification reaction. Therefore, the chemical stability of the aromatic C=O
302 structures made it more likely to survive during the thermal cracking and some
303 aromatic C-O structures may transform to the more stable aromatic C=O structures,
304 resulting in a steady amounts of aromatic C=O structures in char until 900 ˚C where
305 the gasification become intensified. In contrast, for the char gasification in steam
306 atmosphere and CO_2 atmosphere, the aromatic C=O structures would be
307 continuously consumed by the gasifying agent, especially with increasing
308 temperature and thus intensified gasification.

309 In order to clarify the changes in the O-containing structure with the progress of
310 gasification, the absolute amounts of aromatic C-O structures and aromatic C=O
311 structures in char as a function of char yield is shown in Fig. 7. It can be seen that,
312 with the progress of gasification, the amounts of aromatic C-O structures of char
313 from gasification in H_2 was significantly lower than that from gasification in the
314 oxidising atmospheres, indicating that the C-O structures was easier to be consumed
315 in the reducing atmospheres. In addition, as is shown in Fig. 7 (b), the amounts of

aromatic C=O structures decreased with decreasing char yield and not much difference can be seen among the three atmospheres, which means that the consumption of aromatic C=O structures was more likely to be proportional to the progress of gasification both in the O-containing atmosphere and non-O-containing atmosphere. Therefore, the steady amounts of aromatic C=O structures in char with increasing temperature during the gasification in H_2 atmosphere was mainly due to weak gasification reaction at that stage.

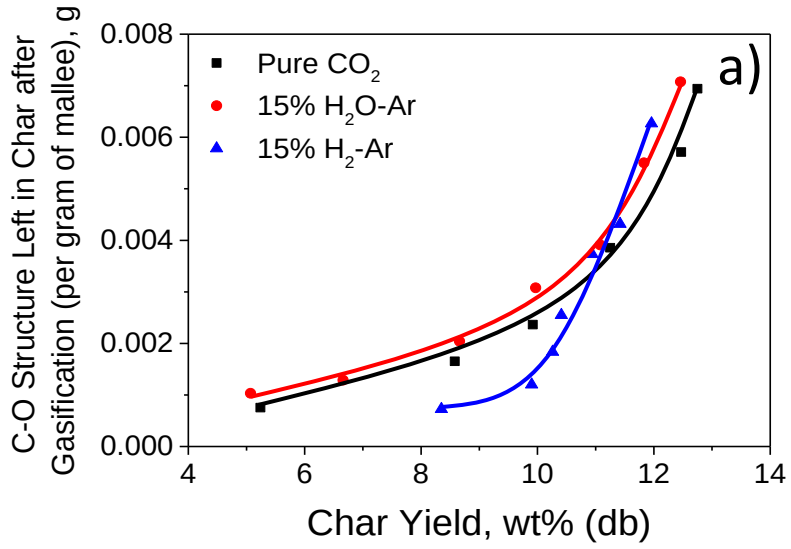

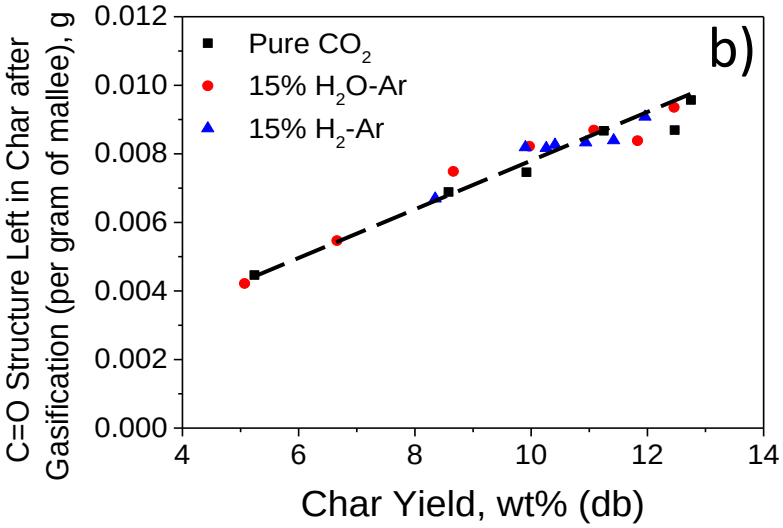

Fig. 7. Amounts of (a) C-O structure and (b) C=O structure left in char after gasification based on per gram of mallee wood obtained by XPS analysis as a function of char yield.

4.6 Oxygenation and de-oxygenation during char gasification

The gasification of low-rank fuels in O-containing atmospheres (e.g. H_2O, CO_2) is an oxygenation process based on our study of the total Raman intensity [4,9]. As mentioned above, the XPS analysis can also give a direct indication of the amount of O species in char during gasification, and it will involve all O species not just the O which have the resonance effect with the aromatic ring to which it is connected.

Fig. 8 illustrates the relative contents of O-containing structure in char with the progress of gasification. The relative contents refer to the contents of each chemical component in char based on per actual gram of biomass char (remaining after gasification). It can be seen that the relative contents of O species of char from gasification in the O-containing atmospheres were higher than that in the non-O-containing atmosphere with the process of gasification. Therefore, it is hypothesised that some O derived from the O-containing gasifying agent leads to the oxygenation of the aromatic ring system in terms of forming some intermediates such as C(CO), C(OH) and C(O) structures in the char matrix during gasification [9,38-41], contributing to the high contents of O species of char.

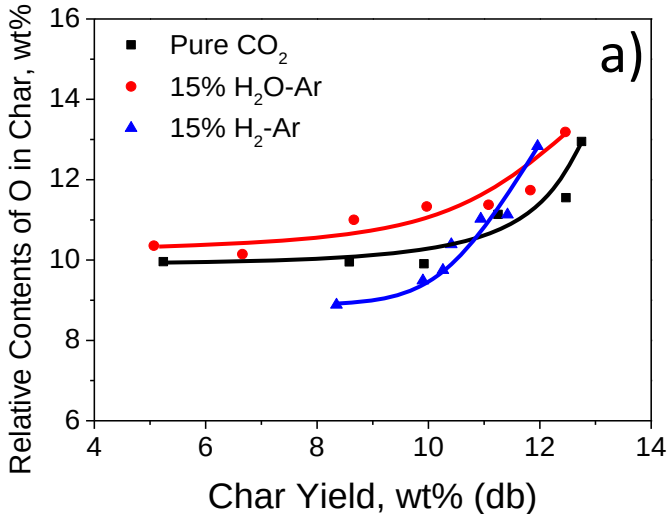

347

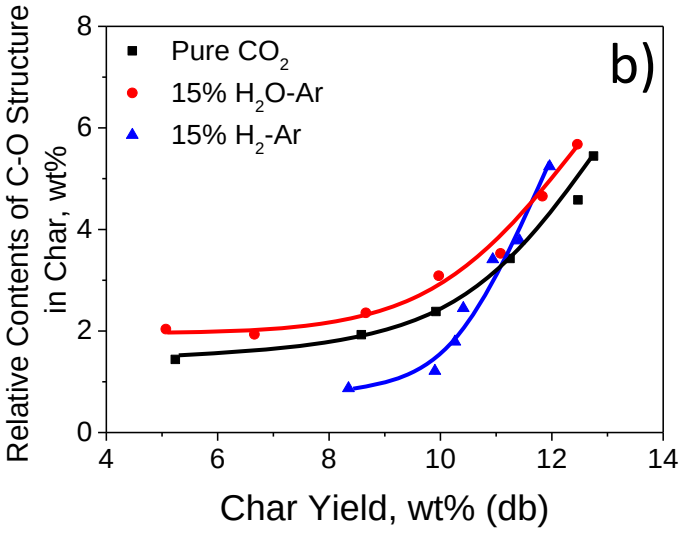

348

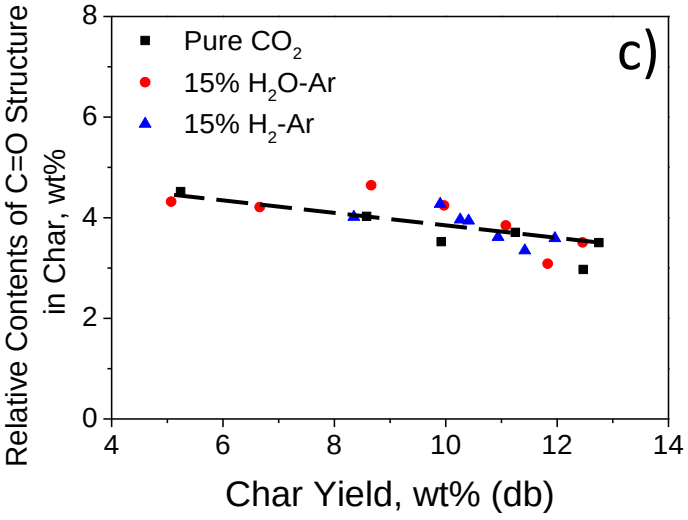

349

350 **Fig. 8.** Relative contents of (a) O species, (b) O with C-O structure and (c) O with C=O structure in
351 char obtained by XPS analysis as a function of char yield.

Further information can be obtained from the deconvolution result of the O 1s spectra. As is shown in Fig. 8 (b) and (c), The contents of aromatic C-O structure of char gasified in the O-containing atmosphere was much higher than that in the non-O-containing atmosphere with the process of gasification, while not much difference can be observed for the contents of aromatic C=O structure among the three atmospheres. All of these indicated that the captured O species from the O-containing gasifying agent were much likely bonded to the char matrix with C-O structure. Furthermore, considering the high gasification rate of char in steam atmosphere and in CO_2 atmosphere as well as our previous studies [4,9] which indicated that some kinds of O-containing structures in char were responsible for enhancing the char gasification rate, the continuously generated C-O structures in the O-containing atmosphere were most likely to be responsible for promoting the char gasification reactivity.

5. Conclusions

Australia mallee wood was gasified in a fluidised-bed reactor at 600-900 ˚C in O-containing atmosphere (pure CO_2, 15% H_2O-Ar) and non-O-containing atmosphere (15% H_2-Ar). Our results revealed that the gasification rate of char in steam atmosphere and CO_2 atmosphere was much higher than that in H_2 atmosphere. For the gasification in CO_2 at 900 ˚C, $CaCO_3$ and $MgCO_3$ would form on char surface. The similar O/C ratio of char from XPS and elemental analysis indicated the chemical similarity between char surface and char matrix. In addition, the aromatic C-O structure in char was highly reactive so that it can be easily removed or broken down while the low reactivity of the aromatic C=O structure made it more likely to

survive during gasification compared with the aromatic C-O structure. The amount of aromatic C-O structure left in the char during gasification in non-O-containing atmosphere was lower than that in O-containing atmosphere, especially at low char yield. In contrast the consumption of aromatic C=O structure was proportional to the progress of gasification, regardless of the atmosphere. Moreover, the high contents of O species in chars with the progress of gasification in steam and in CO_2 confirmed the oxygenation of char gasified in the O-containing atmosphere. The newly formed C-O structure in char during the oxygenation was most likely to be responsible for the high gasification reactivity of char in the O-containing atmosphere.

Acknowledgements

This project received funding from the Australian Government through ARENA's Emerging Renewables Programs. This project was also supported by the Australian Research Council (DP110105514) and the Commonwealth of Australia under the Australia-China Science and Research Fund. The authors also acknowledge the use of equipment, scientific and technical assistance of the WA X-Ray Surface Analysis Facility, funded by the Australian Research Council LIEF grant LE120100026.

References

[1] C.-Z. Li, Special issue-gasification: A route to clean energy, Process Saf. Environ. Prot. 84 (2006) 407-408.

[2] C.-Z. Li, Importance of volatile-char interactions during the pyrolysis and gasification of low-rank fuels – A review, Fuel 112 (2013) 609-623.

[3] C.-Z. Li, Some recent advances in the understanding of the pyrolysis and gasification behaviour of Victorian brown coal, Fuel 86 (2007) 1664-1683.

[4] H.-L. Tay, S. Kajitani, S. Wang, C.-Z. Li, A preliminary Raman spectroscopic perspective for the roles of catalysts during char gasification, Fuel 121 (2014) 165-172.

[5] C.-Z. Li, C. Sathe, J.R. Kershaw, Y. Pang, Fates and roles of alkali and alkaline earth metals during the pyrolysis of a Victorian brown coal, Fuel 79 (2000) 427-438.

[6] D.M. Quyn, H. Wu, S.P. Bhattacharya, C.-Z. Li, Volatilisation and catalytic effects of alkali and alkaline earth metallic species during the pyrolysis and gasification of Victorian brown coal. Part II. Effects of chemical form and valence, Fuel 81 (2002) 151-158.

[7] T. Li, L. Zhang, L. Dong, S. Wang, Y. Song, L. Wu, C.-Z. Li, Effects of char chemical structure and AAEM retention in char during the gasification at 900° C on the changes in low-temperature char-O_2 reactivity for Collie sub-bituminous coal, Fuel 195 (2017) 253-259.

[8] D. Lv, M. Xu, X. Liu, Z. Zhan, Z. Li, H. Yao, Effect of cellulose, lignin, alkali and alkaline earth metallic species on biomass pyrolysis and gasification, Fuel Process. Technol. 91 (2010) 903-909.

[9] T. Li, L. Zhang, L. Dong, C.-Z. Li, Effects of gasification atmosphere and temperature on char structural evolution during the gasification of Collie sub-bituminous coal, Fuel 117 (2014) 1990-1995.

[10] H.-L. Tay, S. Kajitani, S. Zhang, C.-Z. Li, Effects of gasifying agent on the evolution of char structure during the gasification of Victorian brown coal, Fuel 103 (2013) 22-28.

[11] Y. Zhao, D. Feng, Y. Zhang, Y. Huang, S. Sun, Effect of pyrolysis temperature on char structure and chemical speciation of alkali and alkaline earth metallic species in biochar, Fuel Process. Technol. 141 (2016) 54-60.

[12] L. Zhang, S. Kajitani, S. Umemoto, S. Wang, D. Quyn, Y. Song, T. Li, S. Zhang, L. Dong, C.-Z. Li, Changes in nascent char structure during the gasification of low-rank coals in CO_2, Fuel 158 (2015) 711-718.

[13] S. Zhang, Z. Min, H.-L. Tay, M. Asadullah, C.-Z. Li, Effects of volatile–char interactions on the evolution of char structure during the gasification of Victorian brown coal in steam, Fuel 90 (2011) 1529-1535.

[14] X. Li, J.-i. Hayashi, C.-Z. Li, FT-Raman spectroscopic study of the evolution of char structure during the pyrolysis of a Victorian brown coal, Fuel 85 (2006) 1700-1707.

[15] H.-L. Tay, C.-Z. Li, Changes in char reactivity and structure during the gasification of a Victorian brown coal: Comparison between gasification in O_2 and CO_2, Fuel Process. Technol. 91 (2010) 800-804.

[16] H.-L. Tay, S. Kajitani, S. Zhang, C.-Z. Li, Inhibiting and other effects of hydrogen during gasification: Further insights from FT-Raman spectroscopy, Fuel 116 (2014) 1-6.

[17] X. Liu, Y. Zheng, Z. Liu, H. Ding, X. Huang, C. Zheng, Study on the evolution of the char structure during hydrogasification process using Raman spectroscopy, Fuel 157 (2015) 97-106.

[18] S. Wang, T. Li, L. Wu, L. Zhang, L. Dong, X. Hu, C.-Z. Li, Second-order Raman spectroscopy of char during gasification, Fuel Process. Technol. 135 (2015) 105-111.

[19] Y. Sekine, K. Ishikawa, E. Kikuchi, M. Matsukata, A. Akimoto, Reactivity and structural change of coal char during steam gasification, Fuel 85 (2006) 122-126.

[20] X. Guo, H.-L. Tay, S. Zhang, C.-Z. Li, Changes in char structure during the gasification of a Victorian brown coal in steam and oxygen at 800 C, Energy Fuels 22 (2008) 4034-4038.

[21] D.L. Perry, A. Grint, Application of XPS to coal characterization, Fuel 62 (1983) 1024-1033.

[22] S.G. Chen, R.T. Yang, F. Kapteijn, J.A. Moulijn, A new surface oxygen complex on carbon: toward a unified mechanism for carbon gasification reactions, Ind. Eng. Chem. Res. 32 (1993) 2835-2840.

[23] S.D. Gardner, C.S.K. Singamsetty, G.L. Booth, G.-R. He, C.U. Pittman, Surface characterization of carbon fibers using angle-resolved XPS and ISS, Carbon 33 (1995) 587-595.

[24] F. Marquez-Montesinos, T. Cordero, J. Rodriguez-Mirasol, J.J. Rodriguez, CO_2 and steam gasification of a grapefruit skin char, Fuel 81 (2002) 423-429.

[25] A.R. Gonzalez-Elipe, A. Martinez-Alonso, J.M.D. Tascon, XPS characterization of coal surfaces: study of aerial oxidation of brown coals, Surf. Interface Anal. 12 (1988) 565-571.

[26] Y. Qiao, S. Chen, Y. Liu, H. Sun, S. Jia, J. Shi, C.M. Pedersen, Y. Wang, X. Hou, Pyrolysis of chitin biomass: TG-MS analysis and solid char residue characterization, Carbohydr. Polym. 133 (2015) 163-170.

[27] G. Levi, O. Senneca, M. Causa, P. Salatino, P. Lacovig, S. Lizzit, Probing the chemical nature of surface oxides during coal char oxidation by high-resolution XPS, Carbon 90 (2015) 181-196.

[28] A.M. Puziy, O.I. Poddubnaya, R.P. Socha, J. Gurgul, M. Wisniewski, XPS and NMR studies of phosphoric acid activated carbons, Carbon 46 (2008) 2113-2123.

[29] Wang S, Evolution of char structure and reactivity during gasification, dissertation, Curtin University, 2016.

[30] W. Xia, J. Yang, C. Liang, Investigation of changes in surface properties of bituminous coal during natural weathering processes by XPS and SEM, Appl. Surf. Sci. 293 (2014) 293-298.

[31] D. Briggs, G. Beamson, XPS studies of the oxygen 1s and 2s levels in a wide range of functional polymers, Anal. Chem. 65 (1993) 1517-1523.

[32] E. Desimoni, G.I. Casella, A. Morone, A.M. Salvi, XPS determination of oxygen-containing functional groups on carbon-fibre surfaces and the cleaning of these surfaces, Surf. Interface Anal. 15 (1990) 627-634.

[33] S. Glenis, M. Benz, E. LeGoff, J.L. Schindler, C.R. Kannewurf, M.G. Kanatzidis, Polyfuran: a new synthetic approach and electronic properties, J. Am. Chem. Soc. 115 (1993) 12519-12525.

[34] D.M. Quyn, J.-i. Hayashi, C.-Z. Li, Volatilisation of alkali and alkaline earth metallic species during the gasification of a Victorian brown coal in CO_2, Fuel Process. Technol. 86 (2005) 1241-1251.

[35] C.S.M. Lecea, M. Almela-Alarcon, A. Linares-Solano, Calcium-catalysed carbon gasification in CO_2 and steam, Fuel 69 (1990) 21-27.

[36] M.B. Cerfontain, J.A. Moulijn, The interaction of CO_2 and CO with an alkali carbonate carbon system studied by in-situ Fourier Transform infrared spectroscopy, Fuel 65 (1986) 1349-1355.

[37] M. Ni, B.D. Ratner, Differentiating calcium carbonate polymorphs by surface analysis techniques – an XPS and TOF-SIMS study, Surf. Interface Anal. 40 (2008) 1356-1361.

[38] M. Jiang, J. Hu, J. Wang, Calcium-promoted catalytic activity of potassium carbonate for steam gasification of coal char: effect of hydrothermal pretreatment, Fuel 109 (2013) 14-20.

[39] T.-W. Kwon, S.D. Kim, D.P.C. Fung, Reaction kinetics of char-CO_2 gasification, Fuel 67 (1988) 530-535.

[40] K.J. Huttinger, Mechanism of water vapor gasification at high hydrogen levels, Carbon 26 (1988) 79-87.

[41] G. Hermann, K.J. Huttinger, Mechanism of water vapour gasification of carbon – A new model, Carbon 24 (1986) 705-713.